Approximate analytical solutions in a model for highly concentrated granular-fluid flows

Diego Berzi
Department of Environmental, Hydraulic, Infrastructures and Surveying Engineering, Politecnico di Milano, Milan 20133 Italy

James T. Jenkins
Department of Theoretical and Applied Mechanics, Cornell University, Ithaca, New York 14853, USA
(Received 25 February 2008; published 17 July 2008)

We extend a simple two-phase model for a steady fully developed flow of particles and water over an erodible inclined bed to situations in which the water and particles do not have the same depth. The rheology of the particles is based on recent numerical simulations and physical experiments, the rheology of the fluid is based on an eddy viscosity, and the interaction between the particles and the fluid is through drag and buoyancy. Simple approximations permit analytical expressions for the flow velocities and the depth of flow to be obtained that satisfactorily reproduce those measured in experiments.

DOI: 10.1103/PhysRevE.78.011304 PACS number(s): 45.70.−n, 47.55.−t

I. INTRODUCTION

The motion of debris flows has drawn the attention of the scientific community because of the often dramatic physical consequences of such phenomena and the complex interaction between the physical mechanisms that determine their behavior. Debris flows typically consist of unsteady inhomogeneous surges of polydispersed granular-fluid mixtures characterized by erosion and deposition of the solid material at their base. A mathematical description of such flows requires the determination of the resistance to the motion due to frictional contact and collisions between the particles, together with the interactions between particles and fluid. To accomplish this, extremely idealized conditions, such as steady fully developed flows of a roughly monodispersed mixture, can be employed to test the capability of a theory to capture the essential physics of the process.

Recently [1], we proposed a two-phase theory for steady fully developed flows of granular-fluid mixtures over an erodible bed for saturated flows, in which the height of the flowing particles is equal to the height of the flowing fluid. That theory was based on the following assumptions: (i) the divergence of the flux of the fluctuation energy of the particles is negligible, so that a unique relation (particle rheology) between particle stress ratio, concentration, and inertial parameter [2] exists; (ii) most of the flow is characterized by high values of the concentration, so that the particle rheology can be assumed to be linear after an initial yield, as suggested by numerical experiments on disks [3] and spheres [4]; (iii) the inertia of the particles is large enough that, from the micromechanical point of view, the presence of the fluid does not affect the particle interactions; (iv) the presence of the sidewalls influences the flow by providing an additional frictional force [5,6]; (v) the momentum transfer in the fluid can be modeled in a rough way through a mixing length approach; (vi) the interaction between the particles and the fluid is through buoyancy and drag. These assumptions and appropriate boundary conditions were used to obtain a numerical solution.

The introduction of three further approximations: (i) similar shapes of the particle and fluid velocity profiles, (ii) constant mixing length, and (iii) constant concentration in the flow field permitted approximate analytical expressions to be obtained for the particle and fluid velocity profiles, the flow depth, and the inclination of the free surface as a function of the particle and fluid discharge. Good agreement between analytical and numerical solution suggested that the former could be employed in making comparisons with experiments. To obtain the approximate analytical solution, three coefficients, independent of the flow conditions, were required: the yield value of the particle stress ratio at the bed, the Coulomb friction at the sidewalls, and the coefficient of proportionality of the particle stress ratio with the inertial parameter.

The results of the approximate analytical theory were compared with experiments performed on the flow of water and plastic cylinders in a rectangular inclined flume [7]. Unfortunately, only three experiments on saturated flows were reported on by Larcher *et al.* [7]. Nevertheless, the three coefficients of the model could be set through fitting the experimental values of flow depth and mean particle velocity against the inclination of the free surface, and the theory could be employed to reproduce the profiles of particle velocity and stresses in the flow. The fact that the values of the coefficients resulting from the fit were close to those suggested or inferred from previous work on dry granular flow of disks and spheres [3,4,6,8] provided additional support for their choice.

The aim of the present work is to extend the theory to over- and undersaturated flows, in which the height of the flowing particles is, respectively, less than and greater than the height of the flowing fluid. In an oversaturated flow, there is clear fluid above the granular-fluid mixture. In this case, at the upper surface of the granular-fluid mixture, we assume that the grains are free of tractions. In an undersaturated flow, experiments [9,10] show that there is a plug of dry grains above the granular-fluid interface that extends below the interface as a saturated plug. In this case, at the bottom of the saturated plug, we assume that the ratio of the shear stress to the pressure in the particles is at the value associated with yield. Then, an approximate analytical solution for the general case of a steady fully developed debris flow between flat sidewalls and over an erodible bed can be obtained. This allows a complete description of the flow in terms of velocity, stresses, and concentration profiles and also provides the analytical relation between particle (fluid) shear stress at the

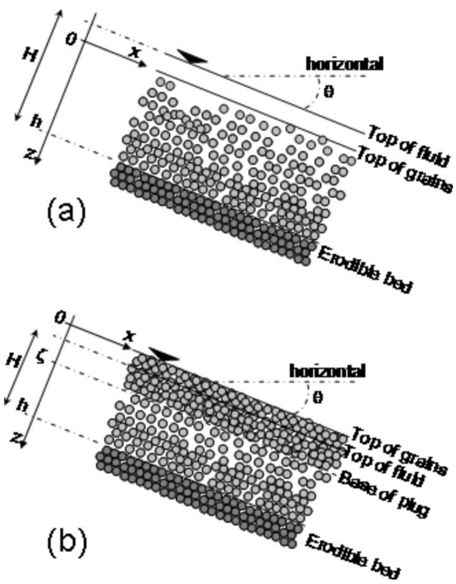

FIG. 1. Sketches of (a) over- and (b) undersaturated debris flows over an erodible bed.

bottom of the flowing layer as a function of the mean particle (fluid) velocity and flow depth.

In Sec. II, we present the balance equations, constitutive relations, and boundary conditions phrased in terms of dimensionless variables; in Sec. III, we derive the approximate analytical theory; in Sec. IV, we compare the predictions of the analytical theory with the experiments reported by Refs. [10,7]; and, finally, in Sec. V, we draw some conclusions.

II. BALANCE LAWS, CONSTITUTIVE RELATIONS, AND BOUNDARY CONDITIONS

Sketches of the geometry of over- and undersaturated debris flows over an erodible bed are shown in Fig. 1. In both cases, we take $z=0$ to be the top of the grains, $z=h$ to be the position of the erodible bed, and H to be the height of the water above the bed. Then, the degree of saturation, $\xi = H/h$ is greater than unity in the oversaturated case and less than unity in the undersaturated. In the undersaturated case, $z=\zeta$ is the total extent of the granular plug.

We let ρ denote the fluid mass density, c the particle concentration, g the gravitational acceleration, θ the free surface inclination, σ the particle specific mass, d the particle diameter, η the fluid viscosity, U the fluid velocity, and u the particle velocity. The Reynolds number $R \equiv \rho d (gd)^{1/2}/\eta$ characterizes the fall velocity of the particles. In what follows, we phrase the momentum balances and constitutive relations in terms of dimensionless variables, with lengths made dimensionless by d, velocities by $(gd)^{1/2}$, and stresses by $\rho\sigma g d$; for simplicity, we denote the dimensionless forms by the same letter as their dimensional counterparts.

We first develop a system of first-order ordinary differential equations and boundary conditions that permit the determination of the profiles of particle and fluid velocity and particle concentration, given the angle of inclination of the bed and the measure ξ of the degree of saturation. Then, rather than solving the resulting system numerically, we introduce simplifying assumptions that permit us to obtain analytical forms of the velocity and concentration profiles. Indeed, our previous work [1] on saturated granular-fluid mixture has already shown that the analytical solution is a good approximation of the numerical one. With either method, knowledge of the velocity and concentration profiles permits the calculation of the volume flow rates of the fluid and the particles. These are the quantities that are usually controlled in an experiment.

A. Fluid momentum balance

The balance of fluid momentum transverse to the flow is

$$P' = \frac{1}{\sigma}\cos\theta, \tag{1}$$

where P is the dimensionless fluid pressure. Here and in the following a prime indicates the derivative with respect to dimensionless z.

The balance of fluid momentum in the direction of flow is

$$S' = (1-c)\frac{1}{\sigma}\sin\theta - \frac{c}{\sigma}C(U-u), \tag{2}$$

where S is the fluid shear stress and C the dimensionless drag:

$$C = \frac{1}{(1-c)^{3.1}}\left(\frac{3}{10}|U-u| + \frac{18.3}{\mathrm{R}}\right). \tag{3}$$

We employ here the expression of the dimensionless drag derived by Dallavalle [9] with the concentration dependence suggested by Richardson and Zaki [11].

Finally, the inverted form of the constitutive relation for the dimensionless shear stress is

$$U' = -\left[\frac{\sigma S}{(1-c)\kappa^2(h-z)^2}\right]^{1/2}. \tag{4}$$

In this differential equation for the fluid velocity, we make the assumption that the mixing length in the turbulent viscosity is proportional to the distance from the bed through Karman's constant, $\kappa=0.41$ [12]. In order to avoid the logarithmic singularity in the velocity profile, we replace the turbulent viscosity with the molecular viscosity where the latter exceeds the former—very close to the bed and, in the undersaturated case, very close to the plug.

B. Particle momentum balance

The balance of particle momentum transverse to the flow is

$$p' = \left(1-\frac{1}{\sigma}\right)c\cos\theta, \tag{5}$$

where p is the dimensionless particle pressure. If W is the dimensionless chute width and μ_w the wall friction, the component of the particle momentum balance parallel to the flow is

$$s' = c \sin \theta + \frac{1}{\sigma} cC(U-u) - 2\frac{\mu_w}{W}p, \quad (6)$$

where s is the dimensionless particle shear stress.

We employ the rheology of the French collaboration GDR MiDi [2] and phrase the particle shear stress in terms of p and an effective coefficient of friction μ,

$$s = \mu p. \quad (7)$$

It has been shown [13] that when the divergence of the fluctuation energy is neglected in the energy balance for the particles, an algebraic relation can be established between the granular temperature (the measure of the particle fluctuations) and the shear rate. In such a case, μ and c are only functions of the inertial parameter, given in terms of the dimensionless variables by

$$I = \frac{|u'|}{(p/\bar{c})^{1/2}}, \quad (8)$$

which can be interpreted as the ratio between the time scales associated with particle motion parellel and perpendicular to the flow, respectively.

Cassar *et al.* [14] have suggested that expression (8) for the inertial parameter is valid only in the freefall regime described by Pont *et al.* [15]. That is when, at the micromechanical level, the particle inertia dominates the fluid drag. This is the case in the experiments performed by Armanini *et al.* [10].

Numerical experiments of simple shear flow of disks [3] and spheres [4] suggest that at high particle concentration the particle rheology can be approximately linear. Therefore, we can express μ as

$$\mu = \check{\mu} + \chi I \quad (9)$$

and c as

$$c = \hat{c} - bI, \quad (10)$$

where $\check{\mu}$, χ, $\hat{c}$, and b are numerical coefficients. The coefficient $\check{\mu}$ is the smallest value of μ for a steady fully developed surface flow in absence of sidewalls and $\hat{c}$ is the corresponding maximum value of the particle concentration.

Upon employing Eqs. (8) and (10), the differential equation for the particle velocity results

$$u' = -\left(\frac{p}{c}\right)^{1/2} \frac{\hat{c} - c}{b}. \quad (11)$$

Finally, from Eq. (9), the algebraic dependence of the concentration on the stress ratio can be obtained,

$$c = \hat{c} - \frac{b}{\chi}\left(\frac{s}{p} - \check{\mu}\right). \quad (12)$$

C. Boundary conditions

One of the main issue concerning granular flows over an erodible bed is the definition of the bed. Recently, Komatsu *et al.* [16] have performed experiments on inclined dry particle flow and they have demonstrated that the definition of the bed as the region where the particles are not moving is not correct. Indeed, if the experiments are carried out over a long enough time, the bed creeps. In other words, a granular flow over an erodible bed is not in equilibrium. However, the experiments performed by Armanini *et al.* [10] are carried out over a much shorter time scale, so that it is reasonable to assume that, at the bed, the particle velocity vanishes,

$$u(h) = 0. \quad (13)$$

This assumption implies that in the bed $u'=0$ and, therefore, from Eqs. (11) and (12),

$$s(h)/p(h) = \check{\mu} \quad (14a)$$

and

$$c(h) = \hat{c}. \quad (14b)$$

A final assumption regarding the boundary conditions at the bed is that the fluid shear stress vanishes there. The study performed by Jenkins and Hanes [12] on dense collisional sheet flows of sediment indicates that at the bed the total shear stress is, indeed, dominated by the momentum transfer due to particle interactions. Hence, at the bed, the gravitational force is balanced only by the drag force,

$$(1-\hat{c})\sin \theta - \hat{c}C(h)U(h) = 0. \quad (15)$$

Equation (15) represents the momentum balance typically employed in groundwater flows [17], where, from Eq. (3),

$$C(h) = \frac{1}{(1-\hat{c})^{3.1}}\left[\frac{3}{10}U(h) + \frac{18.3}{R}\right]. \quad (16)$$

The specification of boundary conditions at the top of the flowing layer requires different treatments for the over- and the undersaturated cases.

In the oversaturated case, we assume that at the interface between the clear fluid and the granular-fluid mixture, $z=0$, both the grain shear stress and the grain pressure vanish. The resulting indeterminate form $s/p=0/0$ is evaluated using L'Hospital's rule:

$$\frac{s(0)}{p(0)} = \lim_{z\to 0}\frac{s'}{p'} = \frac{\sigma}{\sigma - 1}\left[\tan \theta + C(0)\frac{U(0)-u(0)}{\sigma \cos \theta}\right]. \quad (17)$$

In the region of clear fluid of an oversaturated flow, $c=0$ and, as a consequence, $C=0$. At the interface, the shear and normal stresses in the fluid balance the components of the weight of the clear fluid above it,

$$S(0) = \frac{h(\xi - 1)}{\sigma}\sin \theta \quad (18a)$$

and

$$P(0) = \frac{h(\xi - 1)}{\sigma}\cos \theta. \quad (18b)$$

Given the angle of inclination and the degree of oversaturation, the six first-order differential equations (1), (2), (4)–(6), and (11) and the seven boundary conditions (13), (14a), (15), (18a), and (18b) determine $P(z)$, $S(z)$, $U(z)$, $p(z)$, $s(z)$, $u(z)$, and h, while $c(z)$ follows from Eq. (12).

The undersaturated case can be interpreted as a flowing layer of particle and fluid constrained between the bed below and the plug above in which the particles have a solidlike behavior, at least at the time scale of the usual laboratory experiments. The absence of a shear rate in the plug implies that there, as in the bed, the ratio of grain shear stress to the grain pressure is less than or equal to $\check{\mu}$, where the equality applies at the base of the plug,

$$s(\zeta) = \check{\mu} p(\zeta). \tag{19}$$

In the experiments performed by Armanini *et al.* [10], the undersaturated flows are observed at an angle of inclination of the bed much lower that the minimum value for a dry flow. This implies that the plug must extend into the saturated part of the flow. In the dry part of the granular plug, C is absent and $u'=0$; in the saturated part of the plug, the same arguments used for the bed apply and, therefore, $S=0$ and $u'=U'=0$. In Eq. (19), both $p(\zeta)$ and $s(\zeta)$ may then be determined by the balance of forces in the plug:

$$p(\zeta) = \hat{c}\left(1 - \frac{1}{\sigma}\right)[\zeta - h(1-\xi)]\cos\theta + \hat{c}h(1-\xi)\cos\theta, \tag{20}$$

and

$$s(\zeta) = \left\{\zeta + \frac{1}{\sigma}\frac{1-\hat{c}}{\hat{c}}[\zeta - h(1-\xi)]\right\}\hat{c}\sin\theta - \frac{\mu_w}{W}\left\{\zeta^2 - \frac{1}{\sigma}[\zeta - h(1-\xi)]^2\right\}\hat{c}\cos\theta. \tag{21}$$

In the fluid at the base of the plug,

$$S(\zeta) = 0 \tag{22a}$$

and

$$P(\zeta) = \frac{\zeta - h(1-\xi)}{\sigma}\cos\theta. \tag{22b}$$

In this case, the values of both h and ζ must be determined. Given the angle of inclination and the degree of undersaturation, the six first-order differential equations (1), (2), (4)–(6), and (11) and the eight boundary conditions (13), (14a), (15), (19)–(21), (22a), and (22b) determine $P(z)$, $S(z)$, $U(z)$, $p(z)$, $s(z)$, $u(z)$, h, and ζ; while $c(z)$ follows from Eq. (12).

III. APPROXIMATE ANALYTICAL THEORY

As in the saturated case [1], to obtain approximate analytical solutions, we make three fundamental assumptions. First, we simplify the turbulent viscosity in the expression of the fluid shear stress by taking the mixing length to be constant and equal to its average through the flow,

$$S = \frac{1}{\sigma}(1-c)k^2h^2U'^2; \tag{23}$$

where $k=0.20$. Second, we assume that the concentration is constant and at its maximum value,

$$c = \hat{c}. \tag{24}$$

This assumption should be regarded as a first step in an iterative process: once the analytical distribution of the inertial parameter in the flow is obtained, a distribution of the concentration can be derived using Eq. (10) and employed in place of Eq. (24), to determine a more refined approximation of the numerical solution. However, a previous analysis on the saturated case [1] has shown that the first approximation obtained through Eq. (24) is already sufficiently close to the final numerical solution. The third assumption is based on the idea that if the densities of particles and fluid are not so different, as in the experiments of Armanini *et al.* [10], the velocity distributions are expected to be similar. This can be formulated as

$$u' = U'. \tag{25}$$

In order to treat the undersaturated and oversaturated flows in a unified way, we introduce two auxiliary functions of the degree of saturation ξ,

$$\alpha \equiv 1 + \frac{1}{2}(\xi - 1 - |\xi - 1|),$$

$$\beta \equiv 1 + \frac{1}{2}(\xi - 1 + |\xi - 1|). \tag{26}$$

In an undersaturated flow, $\xi<1$, $\alpha=\xi$, and $\beta=1$; while, in an oversaturated flow, $\xi>1$, $\alpha=1$, and $\beta=\xi$. These functions also permit the eventual description of transitions between the two regimes in unsteady situations in a relatively natural way.

We employ the drag force (3) in the particle flow momentum balance (6) and integrate the resulting equation to obtain the distribution of the particle shear stress,

$$s = s^* + \sin\theta\int_{h(1-\alpha)}^{z} c\,dz + \frac{1}{\sigma}\sin\theta\int_{h(1-\alpha)}^{z}(1-c)dz - S + S^* - 2\frac{\mu_w}{W}\int_{h(1-\alpha)}^{z} p\,dz, \tag{27}$$

where s^* and S^* are, respectively, the particle and fluid shear stresses at $z=0$,

$$s^* = h\hat{c}\sin\theta(1-\alpha) - \frac{\mu_w}{W}h^2\hat{c}\cos\theta(1-\alpha)^2 \tag{28}$$

and

$$S^* = \frac{h}{\sigma}\sin\theta(\beta - 1). \tag{29}$$

Similarly, we integrate Eq. (5) to obtain the distribution of the particle pressure,

$$p = p^* + \left(1 - \frac{1}{\sigma}\right)\cos\theta\int_{h(1-\alpha)}^{z} c\,dz, \tag{30}$$

where p^* is the particle pressure at $z=0$; so, with $c=\hat{c}$ in the plug,

$$p^* = h\hat{c}\cos\theta(1-\alpha), \tag{31}$$

and

$$p = \left\{ z - \frac{1}{\sigma}[z - h(1-\alpha)] \right\} \hat{c}\cos\theta. \tag{32}$$

With the approximation (23) for the fluid shear stress and the approximation (24) of constant concentration, the ratio of particle shear stress and pressure is, from Eqs. (27) and (32),

$$\mu = \frac{z + (1/\sigma)(1-\hat{c})[z - h(1-\alpha)]/\hat{c}}{z - (1/\sigma)[z - h(1-\alpha)]}\tan\theta - \frac{1}{\sigma}\frac{1-\hat{c}}{\hat{c}}k^2h^2\xi^2\frac{U'^2}{p/\hat{c}} + \frac{S^*}{\{z - (1/\sigma)[z - h(1-\alpha)]\}c\cos\theta} - \frac{\mu_w}{W}\frac{z^2 - (1/\sigma)[z - h(1-\alpha)]^2}{z - (1/\sigma)[z - h(1-\alpha)]}. \tag{33}$$

This equation provides an explicit characterization, in the context of the approximations, of how the different physical mechanism concur to determine the value of the effective friction. The first term on the right-hand side of Eq. (33) represents the effect of the gravitational force: the apparent weight of the particles in the direction of the flow (numerator) is increased through the drag provided by the interstitial fluid and at the same time the apparent weight in the direction parallel to the flow (denominator) is reduced due to the buoyancy. This results in an increased mobility of the grains which explains why steady fully developed granular-fluid flows are possible at angles much lower than the angle of repose of the dry material. The second term on the right-hand side of Eq. (33) represents the reduction in the drag that the fluid exerts on the particles due to the presence of turbulence. The third term shows that the presence of a layer of clear fluid above the granular-fluid layer increases the value of the effective friction and, therefore, increases the particle mobility. Finally, the last term on the right-hand side of Eq. (33) is the negative contribution of the sidewall friction to the motion. This term is responsible for the association of a unique depth of the flow to a given angle of inclination and a given degree of saturation, as will made clear later in this section.

With the approximation of a constant difference in the particle and fluid velocities [Eq. (25)] and the linear rheology $\mu = \check{\mu} + \chi I$, we rewrite Eq. (33) as

$$\frac{1}{\sigma}\frac{1-\hat{c}}{\hat{c}}(kh\xi I)^2 + \chi I + \frac{\mu_w}{W}\frac{z^2 - (1/\sigma)\hat{z}^2}{z - (1/\sigma)\hat{z}} + \check{\mu} - \frac{z + (1/\sigma)(1-\hat{c})\hat{z}/\hat{c}}{z - (1/\sigma)\hat{z}}\tan\theta - \frac{S^*}{[z - (1/\sigma)\hat{z}]\hat{c}\cos\theta} = 0, \tag{34}$$

where $\hat{z} \equiv z - h(1-\alpha)$, and, from Eq. (8),

$$I = -\frac{u'}{(1-1/\sigma)^{1/2}\{\cos\theta[z + h(1-\alpha)/(\sigma-1)]\}^{1/2}}. \tag{35}$$

Upon taking $I=0$ and $z=h$ in Eq. (34), with S^* given by Eq. (29), we obtain the expression for the particle depth,

$$h = \frac{1}{B}\left[\left(1 - \frac{1}{\sigma}\right)A - \frac{1}{\sigma}(1-\alpha)\left(\frac{1-\hat{c}}{\hat{c}}\tan\theta + \check{\mu}\right) + \frac{1}{\sigma}\frac{\beta-1}{\hat{c}}\tan\theta\right]\left(1 - \frac{1}{\sigma}\alpha^2\right)^{-1}, \tag{36}$$

where

$$A = \frac{\sigma}{\sigma-1}\left(1 + \frac{1}{\sigma}\frac{1-\hat{c}}{\hat{c}}\right)\tan\theta - \mu \quad \text{and } B = \frac{\mu_w}{W}. \tag{37}$$

Upon taking $I=0$ in Eq. (34), we may determine the other value of z, $z=\zeta$ for which $\mu = \check{\mu}$,

$$\zeta^2 + \left(\frac{\chi^2}{4BD} - 2F\right)\zeta + \frac{\chi^2}{4BD}L - N + \frac{\sigma}{\sigma-1}\frac{S^*}{B\hat{c}\cos\theta} = 0, \tag{38}$$

where

$$D = k^2h^2\xi^2\frac{1}{\sigma}\frac{1-\hat{c}}{\hat{c}}, \quad L = h\frac{1-\alpha}{\sigma-1}, \quad F = \frac{\chi^2 + 4AD}{8BD} - L \tag{39}$$

and

$$N = \frac{L}{B}\left[\frac{\chi^2}{4D} - \frac{1-\hat{c}}{\hat{c}}\tan\theta - \check{\mu} + BL(\sigma-1)\right] + \frac{\sigma}{\sigma-1}\frac{S^*}{B\hat{c}\cos\theta}. \tag{40}$$

Equation (38) admits the nontrivial solution only in the undersaturated case,

$$\zeta = -\frac{1}{2}\left(\frac{\chi^2}{4BD} - 2F\right) - \frac{1}{2}\left[\left(\frac{\chi^2}{4BD} - 2F\right)^2 - 4\left(\frac{\chi^2}{4BD}L - N + \frac{\sigma}{\sigma-1}\frac{S^*}{B\hat{c}\cos\theta}\right)\right]^{1/2}. \tag{41}$$

The quadratic Eq. (34) may be solved for I and integrated to obtain the particle velocity profile,

$$\frac{u}{(1-1/\sigma)^{1/2}} = -\frac{\chi(\cos\theta)^{1/2}}{3D}[(h+L)^{3/2} - (z+L)^{3/2}] - \frac{(BD\cos\theta)^{1/2}}{2D}\left[(z-F)(2Fz - z^2 + N)^{1/2} + (F^2+N)\sin^{-1}\left(\frac{z-F}{(F^2+N)^{1/2}}\right)\right] + \frac{(BD\cos\theta)^{1/2}}{2D}\left[(h-F)(2Fh - h^2 + N)^{1/2} + (F^2+N)\sin^{-1}\left(\frac{h-F}{(F^2+N)^{1/2}}\right)\right]. \tag{42}$$

Integrating again between ζ and h, we obtain the mean value of the particle velocity in the flow layer:

$$\frac{u_m}{(1-1/\sigma)^{1/2}} = -\frac{\chi(\cos\theta)^{1/2}}{3D(h-\zeta)}\left[(h+L)^{3/2}h - \frac{2}{5}(h+L)^{5/2} - (h+L)^{3/2}\zeta + \frac{2}{5}(\zeta+L)^{5/2}\right] + \frac{(BD\cos\theta)^{1/2}}{2D}\left[(h-F)(2Fh-h^2+N)^{1/2} + (F^2+N)\sin^{-1}\left(\frac{h-F}{(F^2+N)^{1/2}}\right)\right] - \frac{(BD\cos\theta)^{1/2}}{2D(h-\zeta)}\left\{-\frac{(2Fh-h^2+N)^{3/2}}{3} + \frac{(2F\zeta-\zeta^2+N)^{3/2}}{3} + (F^2+N)^{3/2}\left[\frac{h-F}{(F^2+N)^{1/2}}\sin^{-1}\left(\frac{h-F}{(F^2+N)^{1/2}}\right) + \left(1-\frac{(h-F)^2}{(F^2+N)^{1/2}}\right)^{1/2} - \frac{\zeta-F}{(F^2+N)^{1/2}}\sin^{-1}\left(\frac{\zeta-F}{(F^2+N)^{1/2}}\right) - \left(1-\frac{(\zeta-F)^2}{(F^2+N)^{1/2}}\right)^{1/2}\right]\right\}. \quad (43)$$

In the upper plug layer, $0 \leq z \leq \zeta$, the particle velocity u_p is constant and equal for continuity to $u(\zeta)$.

The volume flux of particles associated with the mean velocity is

$$q = \hat{c}u_m(h-\zeta)W + \hat{c}u_p\zeta W. \quad (44)$$

The constant difference between the fluid and particle velocities can be determined by solving the quadratic equation

$$(U-u)^2 + \frac{18.3}{0.3R}(U-u) - \frac{(1-\hat{c})^{4.1}}{0.3\hat{c}}\sin\theta = 0, \quad (45)$$

that results from the boundary condition (15). In the upper clear water layer, $-h(\beta-1) \leq z \leq 0$, the fluid velocity which results from the turbulent shear stress expression is

$$U = U(0) - \frac{2}{3}\frac{(\sin\theta)^{1/2}}{k\beta h}h^{3/2}(\beta-1)^{3/2} \times\left\{\left[\frac{z}{h(\beta-1)}+1\right]^{3/2} - 1\right\}. \quad (46)$$

The volume flux of fluid can be analytically evaluated through integration of Eqs. (45) and (46).

In conclusion, once the angle of inclination and the degree of saturation are specified, the unique values for the flow depths and volume fluxes of particles and fluid, can be determined. Equivalently, the depths, the inclination and the degree of saturation can be determined if the values of fluid and particle flow rate are given, as in most geophysical and industrial flows. In the following section, we compare the results of the present theory with the experiments performed by Armanini *et al.* [10] and Larcher *et al.* [7].

IV. COMPARISON WITH EXPERIMENTS

Here, we make comparisons with the experiments reported on by Armanini *et al.* [10] and Larcher *et al.* [7] that were carried out in the recirculating flume in which they were able to maintain a steady fully developed flow in a section of the channel. Given the total amount of water and particles (plastic cylinders), a steady fully developed flow was achieved in a section of the channel characterized by a certain inclination of the bed, equal to the inclination of the free surface, but different, in general, from the inclination of the flume. Using image processing techniques, Armanini *et al.* [10] and Larcher *et al.* [7] were able to obtain a detailed description of the flow in terms of the distributions of particle velocity, concentration, granular temperature, and stresses. They provided also a description of the flows in terms of global quantities such as depth and mean particle velocity. However, these quantities were evaluated from depth-averaged momentum and kinetic energy and, as a consequence, the particle velocity at their definition of bed was not negligible. As in our previous work on saturated flows [1], we have reconsidered the data of Larcher *et al.* [7] and evaluated the flow depth as the distance from the free surface at which the granular temperature vanishes. Analogously, the mean velocity has been evaluated through the integration of the velocity profile over our definition of flow depth.

In order to obtain the analytical solutions, we adopt the parameters measured or suggested by Armanini *et al.* [10]. These are $\sigma=1.54$, $d=0.0037$ m, $W=54d$, and $\hat{c}=0.69$. The extremely high value of the concentration at the bed is not unreasonable, given that a partial ordering of the cylindrical particles is expected. For the rheology, we employ the values $\chi=0.5$ and $\check{\mu}=0.41$ and, for the sidewall friction, $\mu_w=0.27$. These values have been obtained through fitting the experiments on saturated flows [1] and are in a good agreement with their corresponding values for dense, dry granular flows [2,3,5,6,8]. To obtain the analytical distribution of the concentration, the parameter b in the particle rheology (10) also has to be specified. Equation (12) shows that, once the value of χ is set, it is possible to evaluate b, if the ratio of the particle shear stress to the particle pressure is known for at least two values of the concentration. We have already found that when $c=0.69$, $\mu=0.41$. In Armanini *et al.* [10], the results of simple shear tests were also reported: for $c=0.58$, the measured value of μ was 0.6. Using this in Eq. (12), leads to a value of b equal to 0.3. Once again, the ratio $b/\chi=0.6$ obtained is in agreement with the corresponding values for dense, dry granular flows of spheres [4] and disks [3] that range between 0.4 and 0.8.

As already mentioned, to obtain the approximate analytical solution, the values of angle of inclination and degree of saturation must be specified. We employed the values measured by Larcher *et al.* [7], but an uncertainty in the degree of saturation has been found for the undersaturated flows, given that the position of the water level in the plug could be influenced by the capillarity. The height of the capillary rise

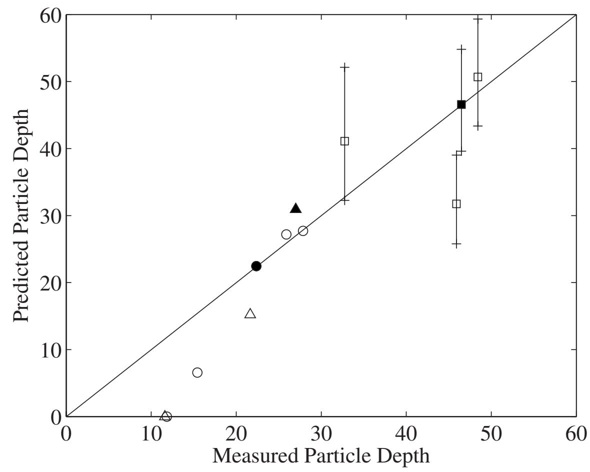

FIG. 2. Predicted versus measured particle depths reported by Larcher *et al.* [7] for oversaturated (triangles), saturated (circles), and undersaturated (squares) flows. The solid line represents perfect agreement. The uncertainty due to the effect of capillarity on the predictions of undersaturated flows is also shown. Filled symbols indicate the experiments used for comparisons in Figs. 4–7.

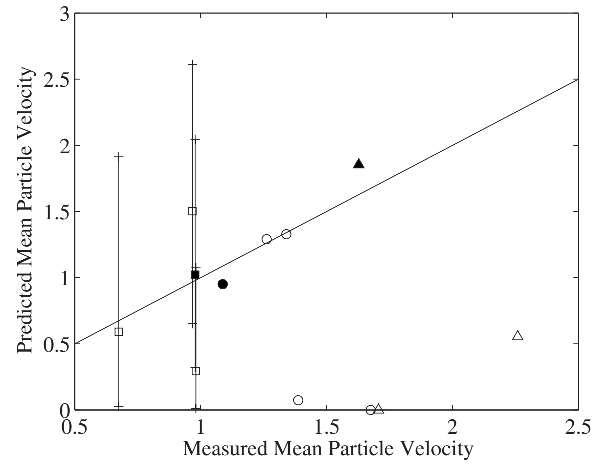

FIG. 3. Predicted versus measured mean particle velocities reported by Larcher *et al.* [7]. Same symbols as in Fig. 2.

has been estimated by Armanini *et al.* [10] to be in the range 5–15 mm. In the following, the results for undersaturated flows refer to a mean correction in the water level of 10 mm, but the extent of the uncertainty is also shown. In Figs. 2 and 3 the values of depth of the particle layer and mean particle velocity are compared with those obtained from the measurements reported on by Larcher *et al.* [7] for 12 runs. When the particle depth is greater than, roughly, 20 diameters, the agreement of the theory with the experiments is remarkable, if the uncertainty due to the presence of capillarity is taken into account. Below this limit, the theory underestimates both the depth and the mean velocity and, in some cases, does not even permit a solution to be obtained. A possible explanation is that the present theory relies on the neglect of the divergence of the fluctuation energy in the energy balance for the particles. Previous analyses [13,18] have shown that this is certainly untrue in a layer of thickness 10 to 15 diameters at the boundaries—in our case, the top of the particle layer and the bed. When the two boundaries are not too far apart and the flow layer is thin, the algebraic relation between granular temperature and shear rate cannot apply, and the theory is expected to fail.

In Figs. 4–7 we show the predictions of the present theory against the experimental data reported by Larcher *et al.* [7] for the distribution over the flow of fluid and particle velocity, concentration, stresses, and granular temperature. Among the datasets provided by Larcher and co-workers, we chose three runs, representative of the three flow conditions deter-

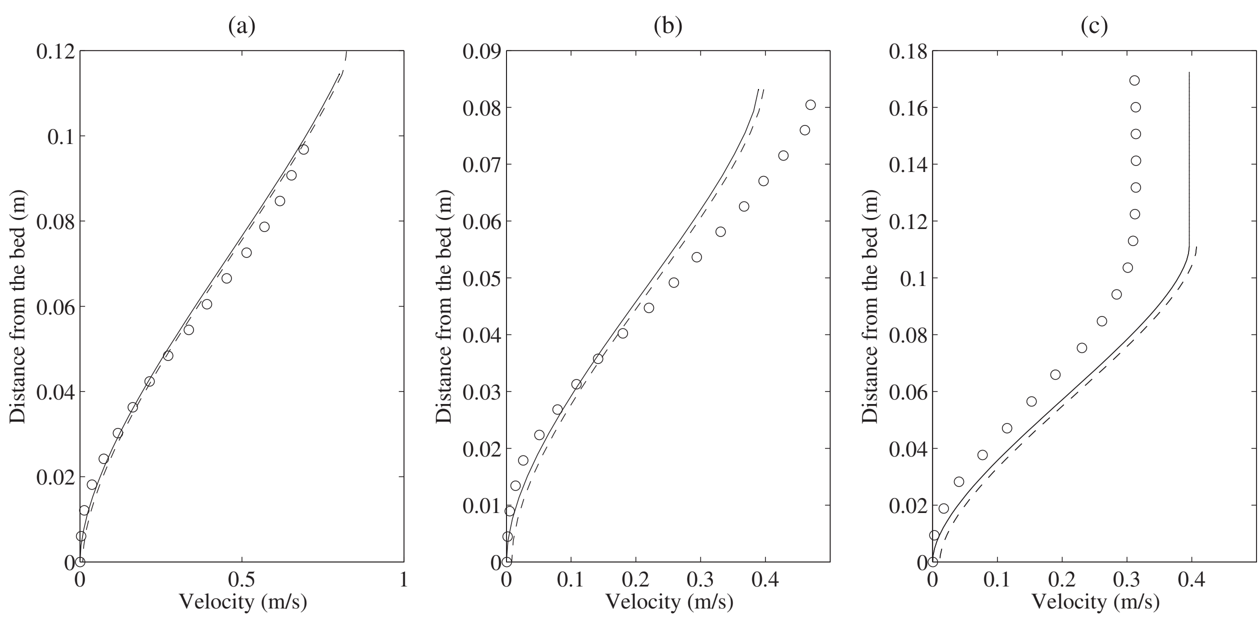

FIG. 4. Predicted velocity profiles for the fluid (dashed line) and the particles (solid line) shown with the measured velocity profile for the particles (open circles) reported by Larcher *et al.* [7]: (a) oversaturated flow with $\theta = 8.5°$ and $\xi = 1.05$; (b) saturated flow with $\theta = 8.1°$ and $\xi = 1.00$; (c) undersaturated flow with $\theta = 12.3°$ and $\xi = 0.91$.

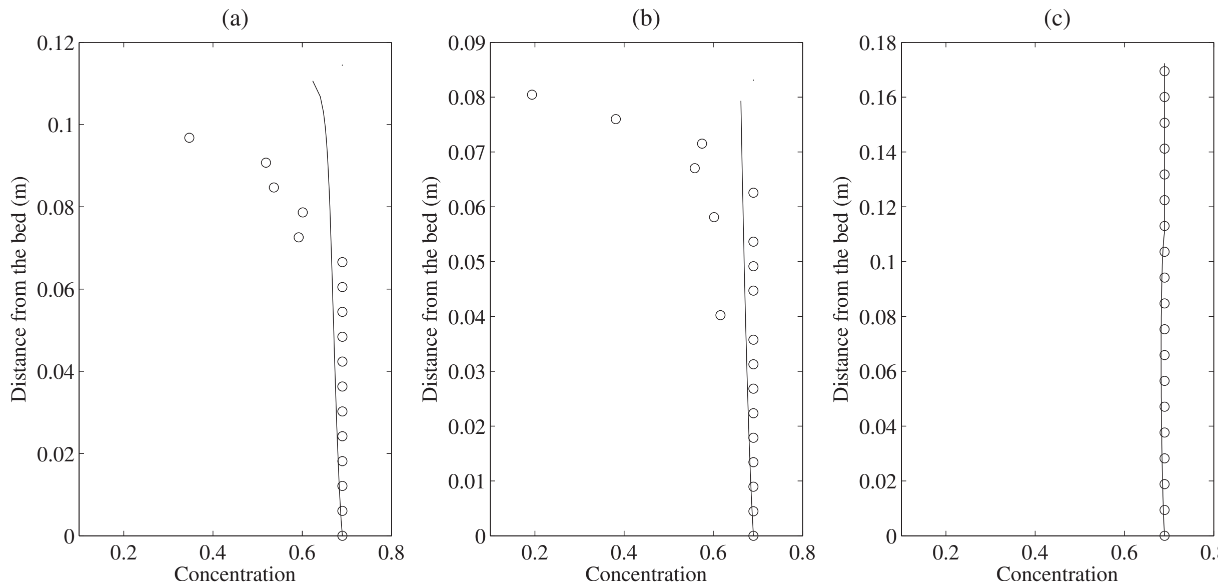

FIG. 5. Predicted (solid line) concentration profiles shown with the measurements (open circles) reported by Larcher *et al.* [7]. Same flow conditions as Fig. 4.

mined by the degree of saturation (respectively, greater, equal, and less than unity).

First, Fig. 4 shows that in addition to the good quantitative agreement with the experiments, our analytical solution is able to satisfactorily reproduce the qualitative features of the experiments: the nonzero derivative of the particle velocity at the top of the particle layer in the oversaturated case [Fig. 4(a)], and the vanishing of u' in the saturated case [Fig. 4(b)]; the correct extent of the plug in the under-saturated case [Fig. 4(c)] and the similarity in the shapes of the velocity profiles, characterized by a change in the concavity. The slight underestimation of the velocity profile in the under-saturated case must be viewed in the context of the uncertainty due to the capillarity effect. There is a less close agreement in a region near the top of the particle layer for the oversaturated and the saturated case: a slight overestimation of the depth in the oversaturated case and an underestimation of the particle velocity in the saturated case. The present theory, as already mentioned, is based on two fundamental assumptions: the flows are dense, and there is an algebraic relation between the square root of the granular temperature and the shear rate.

Figure 5 shows that the lack of agreement in the velocity profiles of Fig. 4 corresponds to a lack of agreement in the concentration profiles and, therefore, also in the distribution of the gravitational contribution to the total shear stress of the mixture (Fig. 6). In the over- and saturated cases, the concentration greatly diminishes in a region close to the top

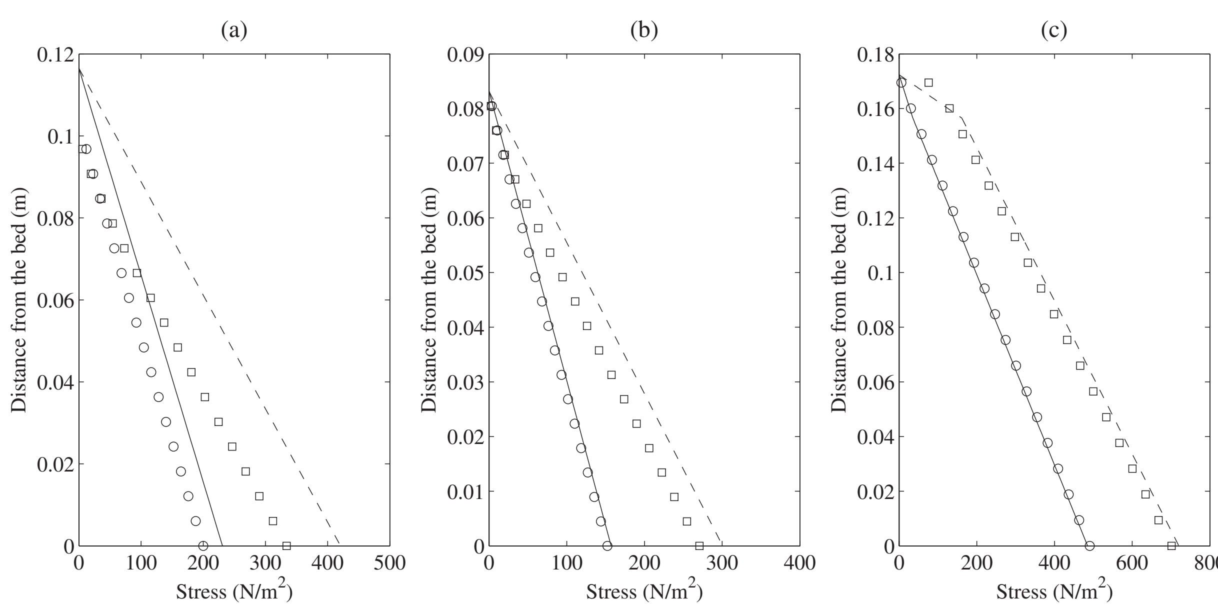

FIG. 6. Predicted (lines) and measured values (symbols, Ref. [7]) of the gravitational contribution to the mixture shear stress (solid line and open circles) and of the particle pressure (dashed line and open squares). Same flow conditions as Figs. 4 and 5.

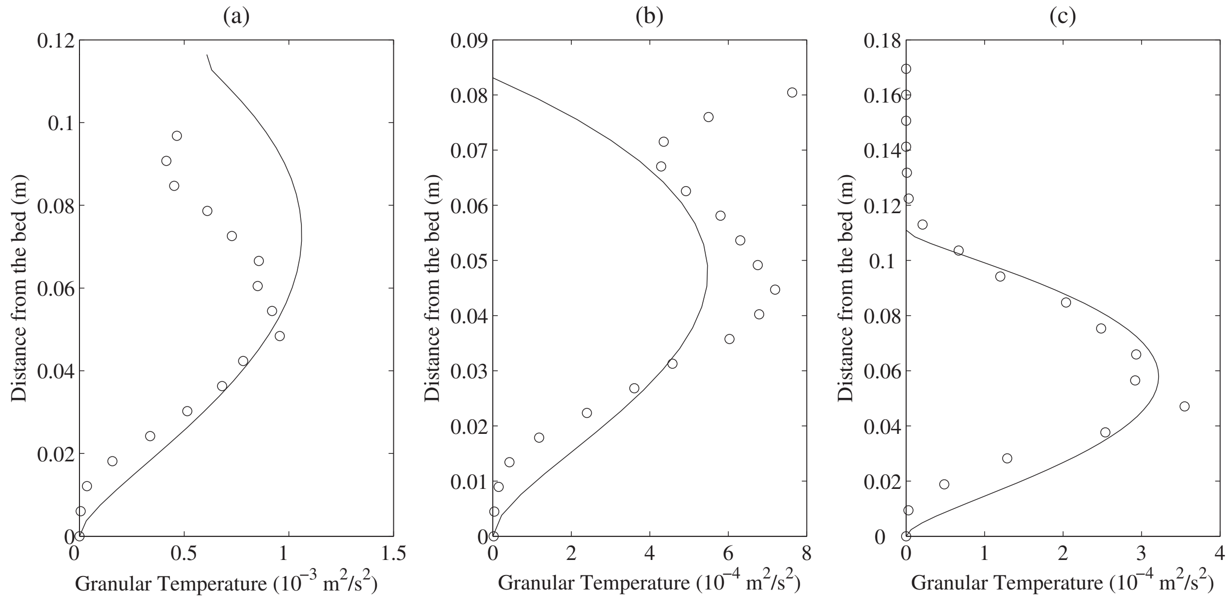

FIG. 7. Predicted values (solid line) of the square of the shear rate times the square of the diameter versus measured values (open circles, Ref. [7]) of the granular temperature. Same flow conditions of Figs. 4–6.

of the particle layer, so that there the flow cannot be considered dense, and the interparticle collisions are essentially binary. Then, the particle rheology is not expected to apply. In Fig. 7, we compare the measured distribution of the granular temperature reported by Larcher *et al.* [7] and our predicted values of the square shear rate, in order to evaluate the neglect of the divergence of the fluctuation energy in the energy balance. Not surprisingly, the agreement is notable for the undersaturated case and also remarkable for saturated and oversaturated cases, except in the region close to the top of the particle layer, where the measurements show an increase in the granular temperature, in contrast to the theory.

V. CONCLUSIONS

We have extended a theory developed for reproducing a steady fully developed flow of a saturated granular-fluid mixture over an erodible bed to the general case in which the height of the particle layer above the bed does not coincide with the height of the fluid. The mixture is treated as a two-phase fluid and we use a linear rheology valid for dense dry granular flows to model the resistance in the particle phase, assuming an algebraic relation between shear rate and square root of the granular temperature. We include the effect of the sidewalls through an additional frictional force and we employ a simple turbulent mixing length approach for determining the fluid shear stress. Finally, we assume that the two phases interact only through buoyancy and drag.

As in the saturated case, we use three further approximations concerning the constancy of mixing length and concentration (at least as a first step in an iterative process) and the similarity of the particle and fluid velocity profiles. This permits a complete analytical solution of the flow to be obtained for global quantities, as depths, mean velocity, angle of inclination, and degree of saturation, and for local quantities, as distributions of fluid and particle velocity, concentration and stresses, given the particle and fluid flow rates. The parameters in the particle rheology and the sidewall friction coefficient have been obtained through fitting with experiments on saturated flows [1], and are characterized by values close to others reported on in literature for dense dry granular flows.

Here, we employ the same values in order to test the general theory against the experimental data of debris flows taken by Armanini *et al.* [10] and Larcher *et al.* [7] in a recirculating flume. The comparisons show that the theory has the capability of reproducing the experimental global quantities of flow depth and mean velocity if the particle layer is not thin, i.e., has a thickness of at least 20 diameters. We claim that this is related to the existence of a region close to upper boundary of the particle layer, in the saturated and oversaturated case, where the divergence of the particle fluctuation energy is not negligible and, therefore, no algebraic relation between shear rate and square root of the granular temperature can be established. When the particle layer is thin, a relevant part of the flow is occupied by this boundary layer and the theory is then expected to fail. This explanation is reinforced by the comparisons with the experiments for the distributions of the local quantities: the lack of agreement in the velocity profiles for saturated and oversaturated flows is in a region close to the top of the particle layer where the concentration is low and there is no correlation between measured granular temperature and predicted square shear rate.

ACKNOWLEDGMENTS

We are grateful to Professor Enrico Larcan for his interest in this work and for his support of our collaboration.

[1] D. Berzi and J. Jenkins, J. Fluid Mech. **608**, 393 (2008).
[2] GDR MiDi, Eur. Phys. J. E **14**, 341 (2004).
[3] F. da Cruz, S. Emam, M. Prochnow, J. N. Roux, and F. Chevoir, Phys. Rev. E **72**, 021309 (2005).
[4] N. Mitarai and H. Nakanishi, Phys. Rev. E **75**, 031305 (2007).
[5] N. Taberlet, P. Richard, A. Valance, W. Losert, J. Pasini, J. Jenkins, and R. Delannay, Phys. Rev. Lett. **91**, 264301 (2003).
[6] P. Jop, Y. Forterre, and O. Pouliquen, J. Fluid Mech. **541**, 167 (2005).
[7] M. Larcher, L. Fraccarollo, A. Armanini, and H. Capart, J. Hydraul. Res. **45**, 59 (2007).
[8] O. Pouliquen, Phys. Fluids **11**, 542 (1999).
[9] J. Dallavalle, *Micromeritics* (Pitman, New York, 1943).
[10] A. Armanini, H. Capart, L. Fraccarollo, and M. Larcher, J. Fluid Mech. **532**, 269 (2005).
[11] J. F. Richardson and W. N. Zaki, Trans. Inst. Chem. Eng. **32**, 35 (1954).
[12] J. Jenkins and D. Hanes, J. Fluid Mech. **370**, 29 (1998).
[13] J. Jenkins, Granular Matter **10**, 47 (2007).
[14] C. Cassar, M. Nicolas, and O. Pouliquen, Phys. Fluids **17**, 103301 (2005).
[15] S. Courrech du Pont, P. Gondret, B. Perrin, and M. Rabaud, Phys. Rev. Lett. **90**, 044301 (2003).
[16] T. S. Komatsu, S. Inagaki, N. Nakagawa, and S. Nasuno, Phys. Rev. Lett. **86**, 1757 (2001).
[17] G. de Marsily, *Quantitative hydrogeology: groundwater hydrology for engineers* (Academic, New York, 1981).
[18] L. E. Silbert, D. Ertas, G. S. Grest, T. C. Halsey, D. Levine, and S. J. Plimpton, Phys. Rev. E **64**, 051302 (2001).